



Article

2-Aminoimidazoles Inhibit *Mycobacterium abscessus* Biofilms in a Zinc-Dependent Manner

Juan M. Belardinelli ¹ , Wei Li ¹, Kevin H. Martin ², Michael J. Zeiler ³, Elena Lian ¹, Charlotte Avanzi ¹ , Crystal J. Wiersma ¹, Tuan Vu Nguyen ⁴, Bhanupriya Angala ¹, Vinicius C. N. de Moura ^{1,†}, Victoria Jones ¹, Bradley R. Borlee ², Christian Melander ^{3,4} and Mary Jackson ^{1,*}

¹ Mycobacteria Research Laboratories, Department of Microbiology, Immunology and Pathology, Colorado State University, Fort Collins, CO 80523, USA; juan.belardinelli@colostate.edu (J.M.B.); wei.li@colostate.edu (W.L.); elian@rams.colostate.edu (E.L.); charlotte.avanzi@colostate.edu (C.A.); crystal.wiersma@colostate.edu (C.J.W.); bhanupriya.angala@colostate.edu (B.A.); caladov@njhealth.org (V.C.N.d.M.); vickijns@gmail.com (V.J.)

² Department of Microbiology, Immunology and Pathology, Colorado State University, Fort Collins, CO 80523, USA; kevhmartin@gmail.com (K.H.M.); brad.borlee@colostate.edu (B.R.B.)

³ Department of Chemistry and Biochemistry, University of Notre Dame, Notre Dame, IN 46556, USA; mzeiler@nd.edu (M.J.Z.); cmelande@nd.edu (C.M.)

⁴ Department of Chemistry, North Carolina State University, Raleigh, NC 27607, USA; tnnguyen@ncsu.edu

* Correspondence: mary.jackson@colostate.edu; Tel.: +1-(970)-491-3582

† Current address: Vinicius Calado Nogueira de Moura, NTM Culture, Biorepository and Coordinating Core, National Jewish Health, Denver, CO 80206, USA.



Citation: Belardinelli, J.M.; Li, W.; Martin, K.H.; Zeiler, M.J.; Lian, E.; Avanzi, C.; Wiersma, C.J.; Nguyen, T.V.; Angala, B.; de Moura, V.C.N.; et al. 2-Aminoimidazoles Inhibit *Mycobacterium abscessus* Biofilms in a Zinc-Dependent Manner. *Int. J. Mol. Sci.* **2022**, *23*, 2950. <https://doi.org/10.3390/ijms23062950>

Academic Editor: Menico Rizzi

Received: 9 February 2022

Accepted: 7 March 2022

Published: 9 March 2022

Publisher's Note: MDPI stays neutral with regard to jurisdictional claims in published maps and institutional affiliations.



Copyright: © 2022 by the authors. Licensee MDPI, Basel, Switzerland. This article is an open access article distributed under the terms and conditions of the Creative Commons Attribution (CC BY) license (<https://creativecommons.org/licenses/by/4.0/>).

Abstract: Biofilm growth is thought to be a significant obstacle to the successful treatment of *Mycobacterium abscessus* infections. A search for agents capable of inhibiting *M. abscessus* biofilms led to our interest in 2-aminoimidazoles and related scaffolds, which have proven to display antibiofilm properties against a number of Gram-negative and Gram-positive bacteria, including *Mycobacterium tuberculosis* and *Mycobacterium smegmatis*. The screening of a library of 30 compounds led to the identification of a compound, AB-2-29, which inhibits the formation of *M. abscessus* biofilms with an IC₅₀ (the concentration required to inhibit 50% of biofilm formation) in the range of 12.5 to 25 μM. Interestingly, AB-2-29 appears to chelate zinc, and its antibiofilm activity is potentiated by the addition of zinc to the culture medium. Preliminary mechanistic studies indicate that AB-2-29 acts through a distinct mechanism from those reported to date for 2-aminoimidazole compounds.

Keywords: *Mycobacterium abscessus*; nontuberculous mycobacteria; biofilm; 2-aminoimidazoles; zinc

1. Introduction

Mycobacterium abscessus subspecies *abscessus* (*Mabs*), *massiliense* (*Mmas*) and *bolletii* (*Mbol*) form a group of opportunistic, rapidly growing mycobacteria that can cause an array of clinical diseases in humans, including lung, skin and soft tissue, central nervous system and disseminated infections. In recent years, the prevalence of pulmonary infections caused by *M. abscessus*, particularly in susceptible individuals with structural or functional lung conditions such as cystic fibrosis (CF), chronic obstructive pulmonary disease (COPD) and bronchiectasis, has been increasing at an alarming rate [1–3]. Treatment for *M. abscessus* pulmonary disease as recommended by the American Thoracic Society and the British Thoracic Society is largely empirical [4,5] and consists of 12–24 months of chemotherapy with a minimum of three antibiotics that lack bactericidal activity and are associated with significant adverse effects [6–8]. Despite aggressive chemotherapy, treatment outcomes remain poor. *M. abscessus* bacteria are indeed the most antibiotic-resistant and antibiotic-tolerant nontuberculous mycobacteria (NTM) owing to their highly impermeable cell envelope and the variety of efflux pumps and drug- and drug-target-modifying enzymes encoded within their genomes [8–10]. Further compounding this problem is the propensity of

M. abscessus to form biofilms [11] and the clinical evidence for *M. abscessus* biofilm formation within the airways and lung cavity of human patients [12–14]. The presence of biofilms, where bacilli are not only shielded from the effect of antibiotics but may also persist in a drug-tolerant state, may help explain why *M. abscessus* lung infections are usually incurable with antibiotic therapy alone and why adjunctive surgical resection of cavities may improve treatment outcome [4].

With the premise that agents capable of inhibiting *M. abscessus* biofilm formation and/or of dispersing established *M. abscessus* biofilms may potentiate the activity of antibiotics used in combination, our attention turned to 2-aminoimidazoles (2-AI). The decision to study 2-AIs was based upon previous studies by the Melander laboratory and others that showed that the 2-AI class of small molecules and related scaffolds (2-aminopyrimidines (2-AP), 2-aminobenzimidazoles (2-ABI), 2-aminoquinazolines and 2-AI-containing meridianin analogs) display broad-spectrum biofilm inhibition and dispersion activity against Gram-negative and Gram-positive bacteria, including *Mycobacterium tuberculosis* and the nontuberculous *Mycobacterium* species, *M. smegmatis* [15–24]. Importantly, some 2-AI and 2-ABI compounds demonstrated the ability to sensitize *M. tuberculosis* and *M. smegmatis* to isoniazid, rifampicin and β -lactams [15,19,23,25].

We here identify a series of 2-AI compounds with the ability to inhibit the formation of *M. abscessus* biofilms with IC_{50} s (the concentration required to inhibit 50% of biofilm formation) in the range of 12.5 to 25 μ M. Interestingly, the lead compound of this series, AB-2-29, is a zinc chelator whose antibiofilm activity is enhanced in the presence of zinc.

2. Results

2.1. Inhibition of *M. abscessus* Biofilm Formation by 2-AI Compounds

To determine whether 2-AI-based small-molecule compounds and related scaffolds inhibited the formation of *M. abscessus* biofilms, we screened a library of 30 compounds, including twenty-six 2-AI analogs, one 2-AP compound (EL-05-047) and three meridianin analogs (7.079; 7.025 and 8.001), of which two contained the 2-AI moiety (Table 1). The screening was conducted using the *Mmas* reference strain CIP 108297 grown as submerged biofilms on poly-D-lysine-coated plates in chemically defined synthetic CF medium (SCFM) as previously described [11]. Recent studies from our laboratory have indeed shown that SCFM closely mimics the nutritional conditions encountered and metabolic adaptation undergone by *M. abscessus* grown in actual CF sputum [26], making this model more relevant to infection than other models based on laboratory media.

Whereas the 2-AP compound and the meridianin analogs failed to show any activity against *Mmas* CIP 108297 biofilms, twelve 2-AI compounds were found to inhibit biofilm formation in a dose-dependent manner and with IC_{50} values at least 2- to 4-fold below their measured MIC in the same medium (Table 1; Figure 1). A subset of these compounds (SEM-002-003; SEM-001-056; SEM-001-050; AB-2-24; AB-2-26, AB-2-29) was retested against other reference and clinical *M. abscessus* isolates encompassing the subspecies *Mabs* and *Mmas* with similar results (Table 1). Subsequent analyses focused on compound AB-2-29, which displayed an IC_{50} less than 4-fold its MIC value. Within the same range of concentrations (6.25 to 50 μ M), however, AB-2-29 was not able to disperse pre-established biofilms (Figure S1).

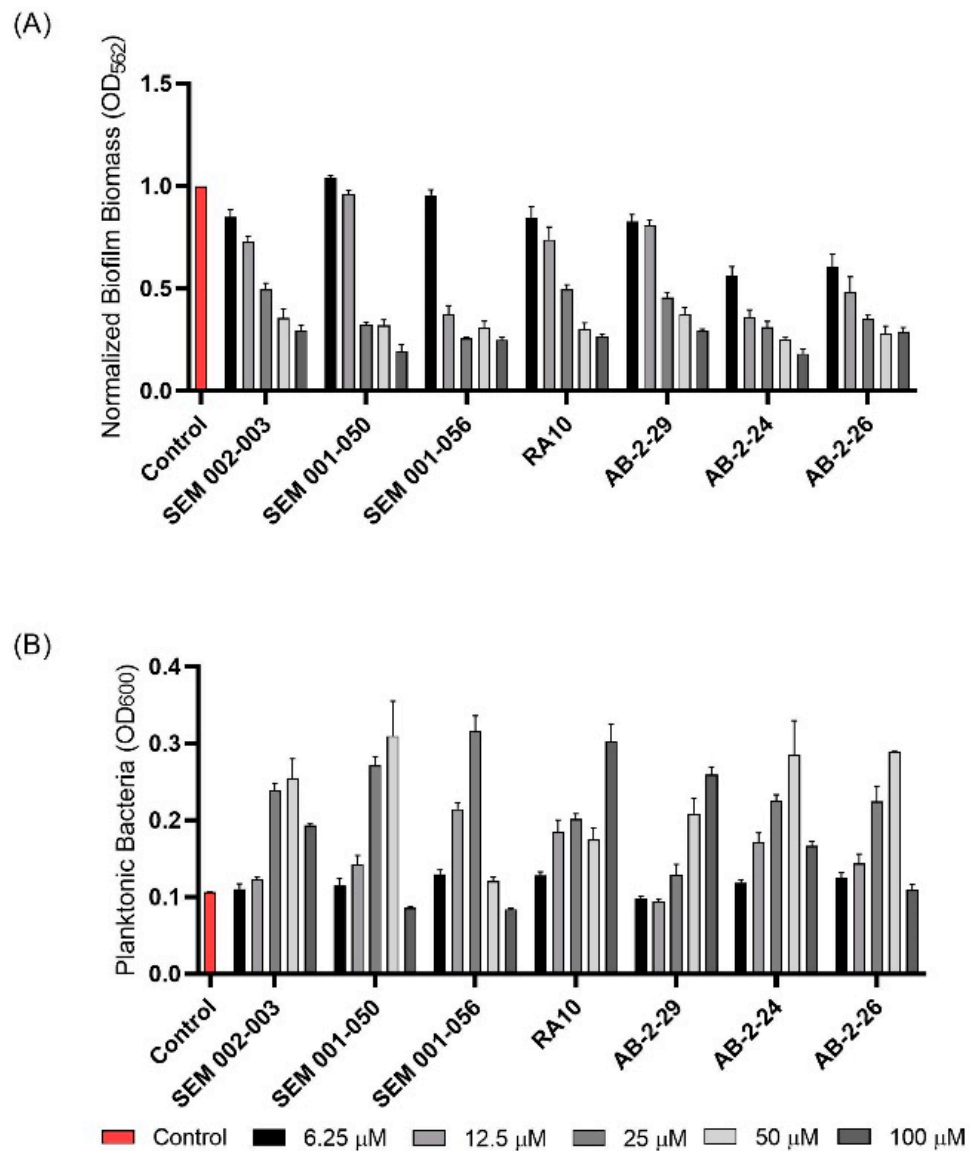


Figure 1. Effect of 2-aminoimidazoles on *M. abscessus* biofilm formation. (A) Biofilm formation of 2-AI-treated *Mmas* CIP 108297 cultures after 5 days of growth in SCFM medium in poly-D-lysine-coated microplates as determined by crystal violet staining. The compounds were added to the culture medium at the indicated concentrations on the first day and maintained throughout the duration of the experiment. The control corresponds to DMSO diluent (0.2% final concentration) without any added 2-AI compound. (B) In parallel, the turbidity of planktonic bacteria released in the medium was assessed spectrophotometrically at 600 nm. Inhibition of biofilm formation correlates with an increase in planktonically growing bacteria in the wells. Decreases in both biofilm and planktonic growth are indicative of the inhibitors having reached their MIC values. The results presented are the means (\pm SD) of quadruplicate wells and are representative of at least two independent experiments.

Table 1. IC₅₀ values for the inhibition of *M. abscessus* biofilms. Biofilm assays and MIC determinations were repeated at least two times. n.d., not determined. MICs were determined against all isolates for which biofilm assays were run. MIC values were the same for all isolates unless otherwise indicated.

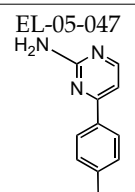
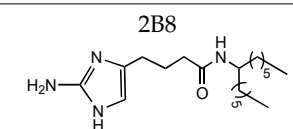
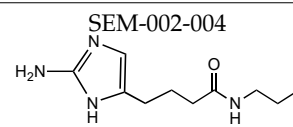
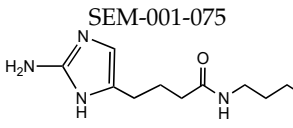
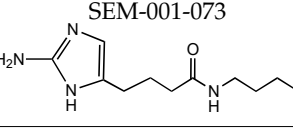
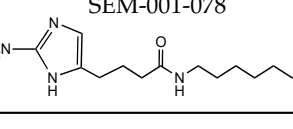
Compound	MIC (M)	IC ₅₀ (M)					
		<i>Mmas</i> CIP 108297	<i>Mabs</i> ATCC 19977	<i>Mabs</i> NJH12	<i>Mmas</i> 1239	<i>Mabs</i> NJH9	<i>Mmas</i> NJH18
EL-05-047 	>100	>100	n.d.	50–100	n.d.	50–100	100
2B8 	25	12.5–25	n.d.	25	n.d.	12.5–25	25
SEM-002-004 	>50	>200	n.d.	n.d.	n.d.	n.d.	n.d.
SEM-001-075 	>50	>200	n.d.	n.d.	n.d.	n.d.	n.d.
SEM-001-073 	>50	>200	n.d.	n.d.	n.d.	n.d.	n.d.
SEM-001-078 	100–200	50	n.d.	n.d.	n.d.	n.d.	n.d.

Table 1. Cont.

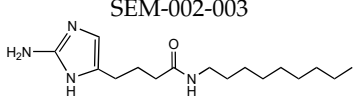
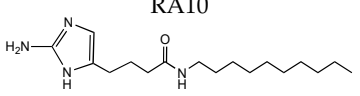
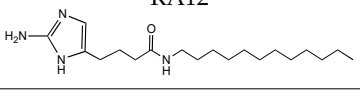
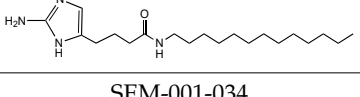
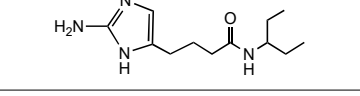
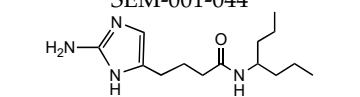
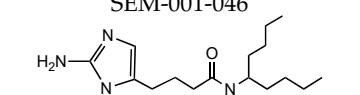
Compound	MIC (M)	IC ₅₀ (M)					
		<i>Mmas</i> CIP 108297	<i>Mabs</i> ATCC 19977	<i>Mabs</i> NJH12	<i>Mmas</i> 1239	<i>Mabs</i> NJH9	<i>Mmas</i> NJH18
SEM-002-003 	50–100 (<i>Mmas</i> CIP 108297 and <i>Mabs</i> ATCC 19977) 50 (<i>Mabs</i> NJH9, <i>Mabs</i> NJH12 and <i>Mmas</i> NJH18)	25	n.d.	12.5–25	n.d.	12.5–25	50
RA10 	>50	25	n.d.	n.d.	n.d.	n.d.	n.d.
RA12 	50	>50	n.d.	n.d.	n.d.	n.d.	n.d.
RA13 	>50	50	n.d.	n.d.	n.d.	n.d.	n.d.
SEM-001-034 	>50	>200	n.d.	n.d.	n.d.	n.d.	n.d.
SEM-001-044 	>50	>200	n.d.	n.d.	n.d.	n.d.	n.d.
SEM-001-046 	100–200	50	n.d.	n.d.	n.d.	n.d.	n.d.

Table 1. Cont.

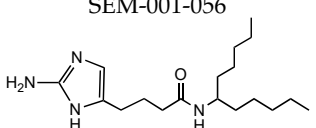
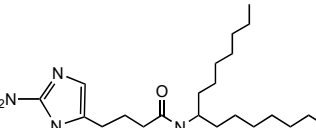
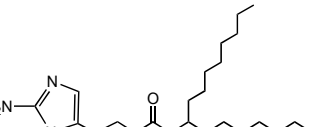
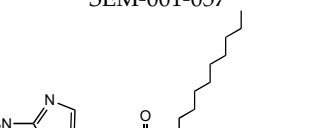
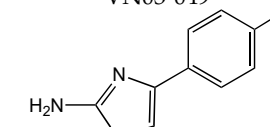
Compound	MIC (M)	IC ₅₀ (M)					
		<i>Mmas</i> CIP 108297	<i>Mabs</i> ATCC 19977	<i>Mabs</i> NJH12	<i>Mmas</i> 1239	<i>Mabs</i> NJH9	<i>Mmas</i> NJH18
SEM-001-056 	50	12.5–25	12.5–25	25	25	12.5–25	25
SEM-001-049 	12.5–25	25	n.d.	n.d.	n.d.	n.d.	n.d.
SEM-001-050 	50 (<i>Mabs</i> NJH9, <i>Mabs</i> NJH12, <i>Mmas</i> NJH18, <i>Mmas</i> CIP108297) 100 (<i>Mabs</i> ATCC 19977)	12.5–25	n.d.	12.5–25	n.d.	12.5–25	12.5–25
SEM-001-057 	50–100	50	n.d.	n.d.	n.d.	n.d.	n.d.
VN03-049 	50–100	25	n.d.	n.d.	n.d.	n.d.	n.d.

Table 1. Cont.

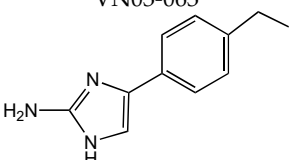
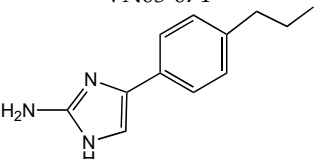
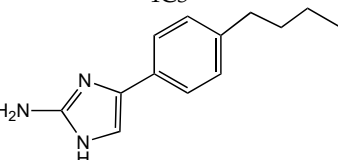
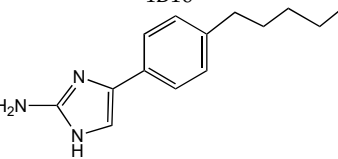
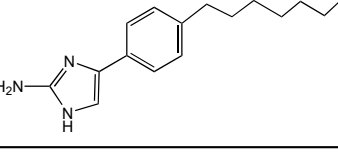
Compound	MIC (M)	IC ₅₀ (M)					
		<i>Mmas</i> CIP 108297	<i>Mabs</i> ATCC 19977	<i>Mabs</i> NJH12	<i>Mmas</i> 1239	<i>Mabs</i> NJH9	<i>Mmas</i> NJH18
VN03-063 	25–50	25	n.d.	n.d.	n.d.	n.d.	n.d.
VN03-074 	50–100	25–50	n.d.	n.d.	n.d.	n.d.	n.d.
4C3 	25–50	12.5	n.d.	n.d.	n.d.	n.d.	n.d.
4B10 	12.5–25	12.5	n.d.	n.d.	n.d.	n.d.	n.d.
4C2 	50	12.5–25	n.d.	n.d.	n.d.	n.d.	n.d.

Table 1. Cont.

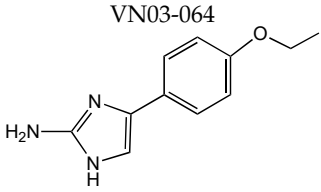
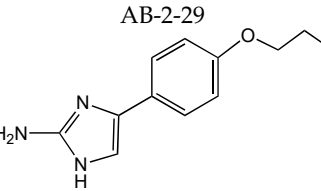
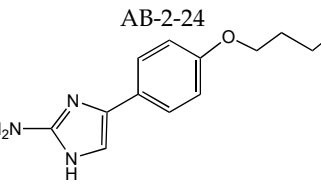
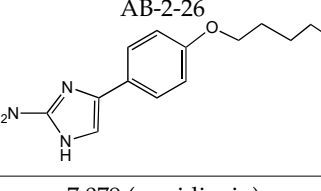
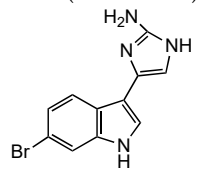
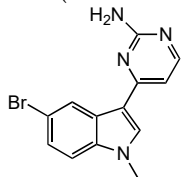
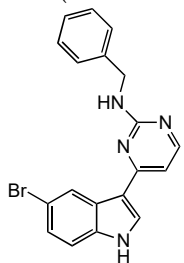
Compound	MIC (M)	IC ₅₀ (M)					
		<i>Mmas</i> CIP 108297	<i>Mabs</i> ATCC 19977	<i>Mabs</i> NJH12	<i>Mmas</i> 1239	<i>Mabs</i> NJH9	<i>Mmas</i> NJH18
VN03-064 	25	25	n.d.	n.d.	n.d.	n.d.	n.d.
AB-2-29 	>100	25	25	12.5–25	50	12.5	25
AB-2-24 	64	12.5	25–50	12.5	25	12.5–25	12.5–25
AB-2-26 	64	12.5–25	25–50	12.5–25	25	6.25–12.5	12.5–25
7.079 (meridianin) 	>100	100	100	50	n.d.	50–100	100

Table 1. Cont.

Compound	MIC (M)	IC ₅₀ (M)					
		<i>Mmas</i> CIP 108297	<i>Mabs</i> ATCC 19977	<i>Mabs</i> NJH12	<i>Mmas</i> 1239	<i>Mabs</i> NJH9	<i>Mmas</i> NJH18
7.025 (meridianin) 	>100	>100	100	50–100	n.d.	>100	50–100
8.001 (meridianin) 	>100	>100	>100	>100	n.d.	>100	>100

2.2. Preliminary Investigations into the Mechanism of Biofilm Inhibition by AB-2-29 in *M. abscessus*

Three main mechanisms of action have thus far been associated with 2-AI compounds and related scaffolds in Gram-positive and Gram-negative bacteria. First is their ability to interfere with two-component signaling systems, resulting in the inhibition and dispersion of *Acinetobacter baumannii*, *Pseudomonas aeruginosa* and *Staphylococcus aureus* biofilms and resensitization of these and other multidrug-resistant bacteria to antibiotics [16,21,27–33]. A second mechanism highlighted by our recent studies in *M. tuberculosis* and *M. smegmatis* relates to the effect of certain 2-AIs on membrane bioenergetics and the proton motive force (PMF) [19,34]. Given the known importance of membrane-mediated anaerobic metabolism in the maintenance of bacterial biofilms [35], this effect of 2-AIs is thought to be the primary driver of their antibiofilm activity in these mycobacterial species. Another report in *A. baumannii* also highlighted the ability of certain 2-AI derivatives to permeabilize bacterial membranes [36].

The ability of AB-2-29 to permeabilize the plasma membrane of *Mabs* subsp. *abscessus* ATCC 19977 was first tested using the LIVE/DEAD BacLight assay, which is based on the nucleic-acid-specific viability dyes propidium iodide and SYTO9. While 0.2 and 0.5% SDS had a dramatic permeabilization effect on the bacilli after one hour of incubation at 37 °C, AB-2-29 failed to show any such effect at its IC₅₀ value (20 µM) (Figure S2).

The ability of AB-2-29 to dissipate the transmembrane potential ($\Delta\Psi$), the transmembrane electrochemical proton gradient (ΔpH) or both components of the PMF in *M. abscessus* was next tested using whole-cell-based and cell-free assays. Impact on the $\Delta\Psi$ and ΔpH of intact *Mabs* ATCC 19977 bacilli grown in SCFM was determined by labeling with 3,3'-diethylloxycarbocyanine iodide (DiOC₂(3)) and 5-chloromethyl-fluorescein diacetate (CMFDA), respectively. As shown in Figure S3, treating the bacilli with 5 or 20 µM of AB-2-29 for 4 h had no significant impact on either the intracellular pH or the $\Delta\Psi$ of *M. abscessus*. A slight but significant effect on $\Delta\Psi$ (but not on intracellular pH) only manifested at the highest concentration of AB-2-29 tested (100 µM; i.e., 5 times its antibiofilm IC₅₀ value). Consistent with these results, AB-2-29 also failed to dissipate the ΔpH of *Mabs* inverted membrane vesicles in a succinate-driven proton translocation assay with the fluorescent substrate ACMA (Figure S4). In conclusion, at concentrations where biofilm formation was inhibited, AB-2-29 did not dissipate the PMF of *M. abscessus*.

2.3. Alteration of *M. abscessus* Response to Zinc Starvation by AB-2-29

As an unbiased approach to gain insight into the mechanism of action of AB-2-29, we next turned to RNA sequencing (RNAseq) to determine the changes undergone by the transcriptional profile of *Mabs* upon exposure to AB-2-29. Duplicate samples of exponentially growing *Mabs* ATCC 19977 cells in SCFM were exposed to 20 µM of AB-2-29 or 0.2% DMSO control for 3 or 24 h at 37 °C with shaking. A comparison of the transcriptional profiles of DMSO- and AB-2-29-treated bacilli at the 3 and 24 h time points was next conducted, and the list of differentially expressed (DE) genes (\log_2 fold-change > 2 with a false discovery rate adjusted $p < 0.05$) is presented in Table S1.

This analysis revealed 40 and 52 upregulated genes and 93 and 51 downregulated genes when comparing DMSO- versus AB-2-29-treated cells after 3 h and 24 h, respectively. A very clear pattern that emerged was a strong (>2.4 to 10.5 \log_2 -fold) downregulation of genes required for adaptation to zinc starvation in the AB-2-29 treatment groups, both at the 3 and 24 h time points. Indeed, at both time points, all 32 predicted Zur regulon genes of *M. abscessus* were expressed at a significantly lower level in the AB-2-29-treated bacilli (Table 2; Figure 2). Other DE genes at both time points were few and essentially encompassed genes involved in lysine and cobalamin biosynthesis, glyoxylase/bleomycin resistance, a β -lactamase gene and genes encoding a number of hypothetical proteins of unknown function. RNAseq analyses otherwise failed to reveal any two-component system regulators among the DE genes, suggesting that AB-2-29 may act differently from other prototypical 2-AIs in inhibiting *M. abscessus* biofilm formation.

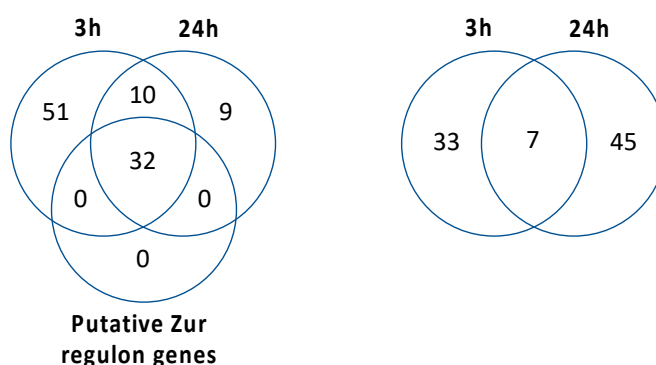
Table 2. List of Zur regulon genes that were expressed at higher or lower levels upon treatment with AB-2-29 compared to DMSO control. Differentially expressed genes upon treatment with 20 μ M AB-2-29 for 3 or 24 h were defined as ≥ 2 log₂ fold-change in expression compared to cells treated with 0.2% DMSO for the same amount of time, with a false discovery rate adjusted *p*-value (*padj*) < 0.05. Genes harboring a *zur-box* in their promoter (see Figure 2B) are marked with an asterisk. Similarly colored genes denote gene clusters likely to be cotranscribed. MAB_0331c, MAB_0332c, MAB_0333c, MAB_0334c and MAB_0336 are Zn-independent alternative ribosomal proteins. MAB_0335 is likely to be involved in cobalamin biosynthesis. MAB_0575c-MAB_0576c-MAB_0577c encode a putative zinc importer of the ABC-transporter family. The operon encompassing genes MAB_1680 to MAB_1701 encodes putative Zn-siderophore biosynthesis and transport proteins, including a putative ABC-transporter and an MCE family transporter.

Gene	Description	Putative Function	Log ₂ Fold-Change	
			AB-2-29 vs. Ctrl 3 h	AB-2-29 vs. Ctrl 24 h
MAB_0331c	30S ribosomal protein S18 RpsR2	Zn-independent ribosomal proteins	−8.04	−9.31
MAB_0332c	30S ribosomal protein S14 RpsN2		−7.76	−8.93
MAB_0333c	50S ribosomal protein L33 RpmG1		−9.72	−6.26
MAB_0334c *	50S ribosomal protein L28 RpmB2		−9.30	−7.83
MAB_0335 *	Probable cobalamin synthesis protein	Cobalamin biosynthesis	−7.95	−10.46
MAB_0336	50S ribosomal protein L31 type B	Zn-independent ribosomal protein	−8.52	−9.38
MAB_0575c	Putative ABC-transporter transmembrane protein	ZnuABC transporter (Zn import)	−2.91	−2.39
MAB_0576c	Putative ABC-transporter ATP-binding protein		−4.05	−2.89
MAB_0577c *	Putative ABC-transporter solute binding protein		−5.54	−5.40
MAB_0809c *	Conserved hypothetical PPE family protein	Unknown	−5.77	−4.66
MAB_1680 *	Hypothetical protein	Zn-siderophore biosynthesis and transport	−9.76	−8.14
MAB_1681	Hypothetical protein		−9.84	−7.80
MAB_1682	Probable NAD-dependent epimerase/dehydratase		−9.04	−8.69
MAB_1683	Putative fatty acid desaturase		−10.30	−7.96
MAB_1684	Diaminobutyrate-2-oxoglutarate aminotransferase		−9.48	−8.31
MAB_1685	Putative decarboxylase		−7.35	−7.01
MAB_1686	Hypothetical protein		−8.48	−7.31
MAB_1687	Hypothetical protein		−8.09	−8.20
MAB_1688	Hypothetical protein		−7.85	−7.90
MAB_1689	Probable ABC-transporter ATP-binding subunit DrrA		−7.99	−7.48
MAB_1690	Putative ABC-transporter transmembrane protein		−8.82	−6.46
MAB_1691	Hypothetical protein		−9.86	−8.31
MAB_1692	Putative polyketide synthase Pks16/acyl-CoA synthetase		−7.95	−7.05
MAB_1693	Conserved hypothetical protein (YrbE family?)		−8.46	−7.52

Table 2. Cont.

Gene	Description	Putative Function	Log ₂ Fold-Change	
			AB-2-29 vs. Ctrl 3 h	AB-2-29 vs. Ctrl 24 h
MAB_1694	Putative YrbE family protein		−8.65	−6.58
MAB_1695	Putative Mce family protein		−8.60	−5.87
MAB_1696	Putative Mce family protein		−7.56	−6.09
MAB_1697	Putative Mce family protein		−7.06	−6.29
MAB_1698	Putative Mce family protein		−7.13	−5.57
MAB_1699	Putative Mce family protein		−7.33	−4.90
MAB_1700	Putative Mce family protein		−6.82	−5.02
MAB_1701	Hypothetical protein		−5.82	−3.61

The “zinc uptake regulator” Zur is the most widespread zinc-responsive transcriptional factor in prokaryotes [37]. In mycobacteria as in most other prokaryotes, Zur transcriptional regulators act as repressors when Zn²⁺ is not limiting in the culture medium. Under these conditions, Zn²⁺ ions become bound to Zur, enabling the protein to bind a *zur-box* in the promoter region of a number of genes, which results in the blockage of the binding site for the RNA polymerase transcription initiation complex. Under low-zinc conditions, Zur dissociates from the *zur-box* derepressing the transcription of a variety of genes involved in Zn²⁺ uptake and the production of zinc-independent enzymes (including zinc-independent ribosomal proteins), among others [37–39]. In our study, the strong expression of Zur-regulated genes in DMSO-treated cells was not unexpected given the absence of added zinc in the SCFM medium used to culture *Mabs* ATCC 19977 (Table S1; Table 2; Figure 2). The fact that the level of expression of these genes considerably decreased in the AB-2-29-treated bacilli was thus indicative of either the presence of zinc brought into the medium by the inhibitor itself or of the ability of the inhibitor to block the Zur repressor in a DNA-binding (i.e., repressing) conformation, even in the absence of zinc in the medium.

(A) Downregulated genes (log₂FC<2) Upregulated genes (log₂FC>2)

(B)

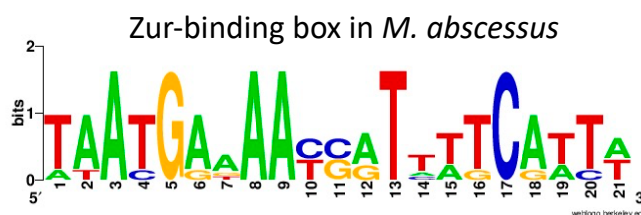


Figure 2. Transcriptional response of *M. abscessus* to AB-2-29 exposure. (A) Venn diagrams showing the number of genes expressed at a significantly higher or lower level in *Mabs* ATCC19977 upon

exposure to 20 μM AB-2-29 for 3 and 24 h compared to DMSO-treated bacilli, and the number of genes among these that are predicted to belong to the *M. abscessus* Zur regulon. The complete list of these genes is provided in Table S1. (B) Consensus sequence logo for predicted *M. abscessus* Zur-binding sites. The *Mabs* ATCC 19977 genome was scanned using the Pattern Locator online software [40] for the presence of putative *Mycobacteriaceae* Zur-binding sites, as defined by Mikhaylina et al. [37] (TRWYGRNAAYSRTN NNCRWYW), in intergenic regions and allowing for up to one mismatch. The search retrieved six binding sites potentially regulating 32 genes, which we defined as Zur regulon genes. The sequence logo for the consensus Zur-binding motif in *Mabs* was constructed using WebLogo [41].

2.4. AB-2-29 Binds Zinc

To differentiate between these two hypotheses, we first sought to determine whether AB-2-29 bound zinc, especially since there was precedence for compounds based on the related 2-aminobenzimidazole scaffold inhibiting *Staphylococcus aureus* biofilms through their ability to chelate zinc from the medium [42,43]. Atomic absorption spectroscopy and NMR-based [44] analyses both converged to indicate that AB-2-29 binds zinc (Figure 3). In contrast, the inhibitor did not bind Fe^{2+} (Figure S5). Per atomic absorption spectroscopy analysis, 0.126 moles of Zn^{2+} came with every one mole of the AB-2-29 batch used in our experiments.

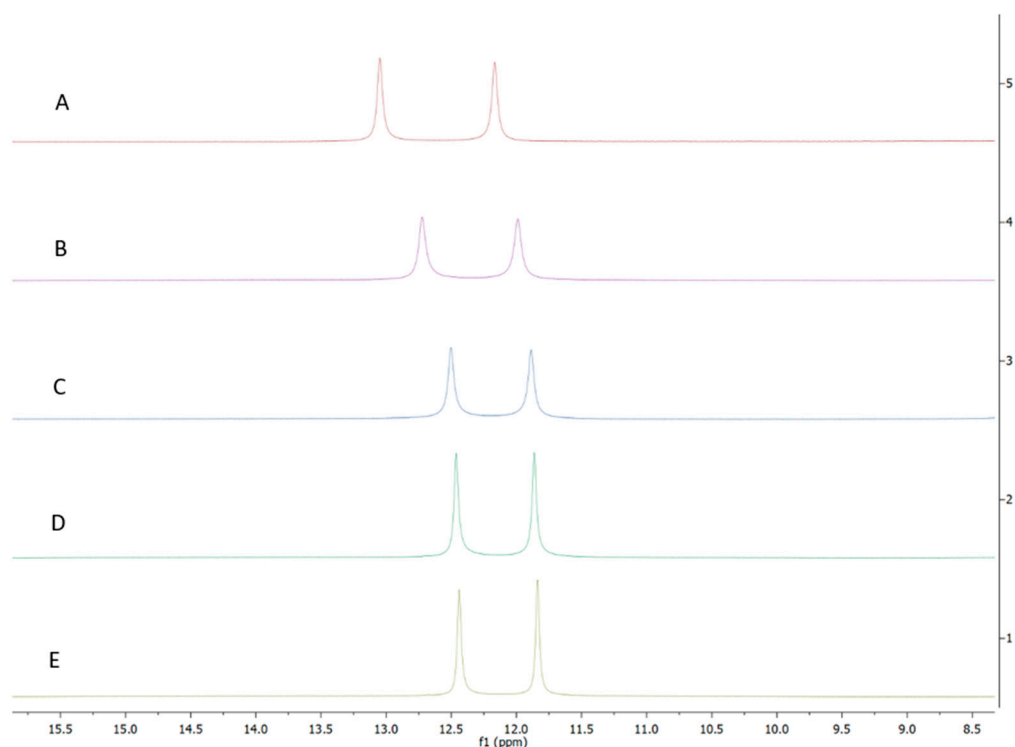


Figure 3. ^1H NMR spectra of AB-2-29 with (A) 0.0 (B) 0.5 (C) 1.0 (D) 2.0 (E) 4.0 equivalents of zinc. The shifting of the NH_2 peaks (between 11.5 and 13.0 ppm) with increased equivalents of zinc implies complexation between AB-2-29 and zinc.

Since Zn^{2+} ions are naturally absent from SCFM, where *M. abscessus* forms abundant biofilms, one can exclude that AB-2-29 prevents biofilm formation by acting as a zinc chelator. Likewise, we exclude that the amount of zinc that comes with AB-2-29 (2.52 μM of zinc at its IC_{50} value of 20 μM) is responsible for the observed antibiofilm activity of this compound, since we previously established that much higher concentrations of zinc were required to inhibit *M. abscessus* biofilm formation in SCFM (IC_{50} of zinc ~150 μM against

Mabs NJH12) [11]. The fact that AB-2-29 comes with small quantities of zinc, however, explains the repression of *zur* regulon genes in AB-2-29-treated cultures.

2.5. Potentiation of the Biofilm Inhibitory Properties of AB-2-29 by Zinc

Given the zinc-binding properties of AB-2-29, we next sought to determine how the presence of zinc in the medium affected the activity of the inhibitor. To this end, biofilm assays were repeated in the absence or presence of different concentrations of ZnSO₄ in SCFM. The results, which are presented in Figure 4A, showed a striking potentiation of the antibiofilm activity of AB-2-29 against three different *Mabs* and *Mmas* strains in the presence of zinc. Since the same treatments did not noticeably impact bacterial growth (with the exception of *Mmas* CIP108297 whose growth rate was slightly reduced in the presence of 20 μM AB-2-29), one can exclude that the reduction in biofilm formation observed in the AB-2-29 +/- Zn²⁺-treated groups was in fact the result of growth inhibition (Figure 4B).

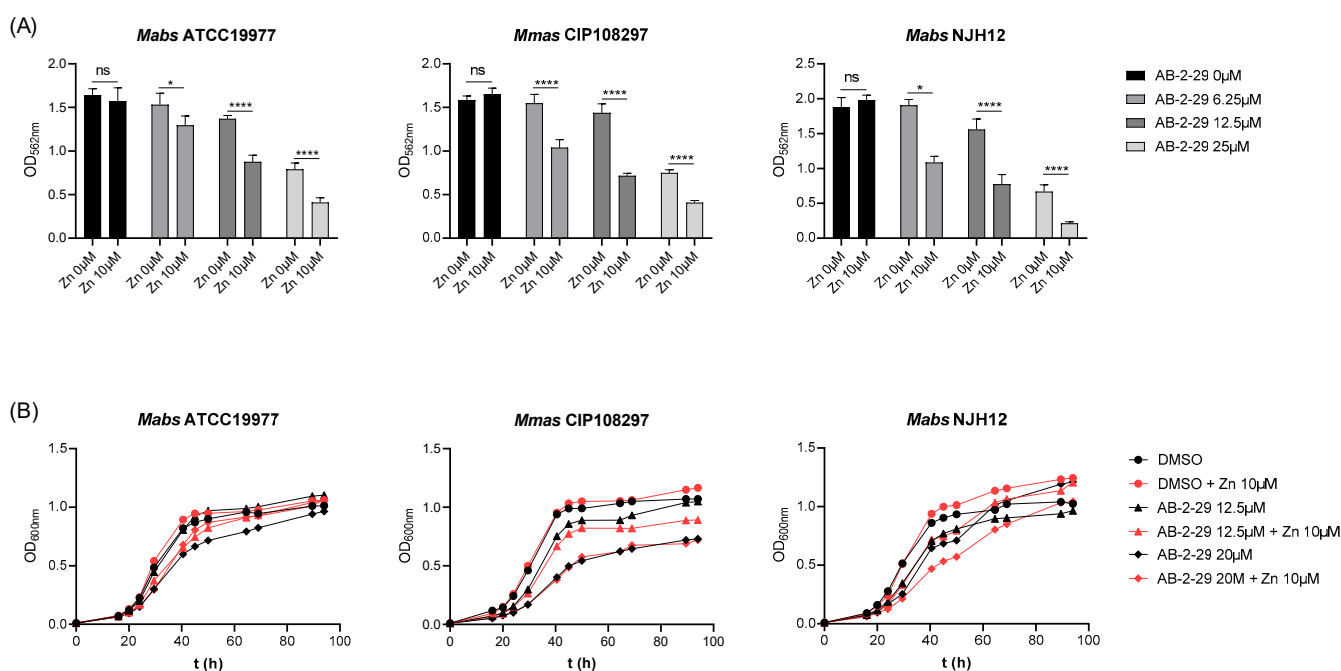


Figure 4. Potentiation of the antibiofilm activity of AB-2-29 by zinc. (A) Biofilm formation by *Mabs* ATCC 19977, *Mabs* NJH12 and *Mmas* CIP108297 in SCFM after 5 days of incubation in the presence or absence of AB-2-29 (0, 6.25, 12.5 or 20 μM) and zinc (0 or 10 μM). The results presented are the means (±SD) of sextuplicate wells and are representative of at least two independent experiments. Asterisks denote statistically significant differences between biofilm inhibitor treatment with and without zinc (* $p < 0.05$ and **** $p < 0.00005$); ns: not significant. (B) Growth of *Mabs* ATCC 19977, *Mabs* NJH12 and *Mmas* CIP108297 in SCFM in the presence or absence of AB-2-29 (0, 6.25, 12.5 or 20 μM) and zinc (0 or 10 μM). The results presented are representative of at least two independent experiments.

3. Discussion

A novel inhibitor of *M. abscessus* biofilm formation has been identified that not only binds to zinc but whose activity also increases in the presence of zinc. The precise mechanism(s) underlying the antibiofilm activity of AB-2-29 and its potentiation by zinc remain(s) to be determined. Unlike previously reported 2-AI compounds and related scaffolds with antibiofilm activity against other Gram-negative or Gram-positive bacteria [16,19,21,27–34,36], AB-2-29 does not appear to act by dissipating the proton motive force or by permeabilizing the plasma membrane of *M. abscessus*. Likewise, no clear evidence could be derived from our RNAseq studies that AB-2-29 interfered with a particular two-component regulatory system in *Mabs* ATCC 19977, although one cannot exclude that such a mechanism is at play. Although the amount of zinc brought by AB-2-29 to the cul-

ture medium is not sufficient to explain, by itself, the antibiofilm activity of this compound, one may speculate that the complexation of zinc by AB-2-29 facilitates the penetration of the inhibitor inside the cells. Alternatively, the repression of Zur regulon genes caused by AB-2-29 may contribute, at least in part, to its activity. Indeed, the zinc-independent ribosomal proteins S18, S14, L33 and L28 have been involved in biofilm formation in *M. smegmatis* [45]. Moreover, we note that a number of genes that are downregulated upon exposure to AB-2-29 (*MAB_1044c*, *MAB_1046c*, *MAB_2204*, *MAB_2706c*, *MAB_3438* and the Zur-regulated Mce operon encoded by the gene cluster encompassing *MAB_1680* to *MAB_1701*) were found to be upregulated in *M. abscessus* during biofilm development [11]. Clearly, further studies are needed to assess the relative contribution of these genes, either individually or combined, to the biofilm-forming capacity of *M. abscessus*. The importance of such studies resides in their potential to lead to better targeted strategies to inhibit *M. abscessus* biofilm formation during infection.

Interestingly, AB-2-29 is not the first example of a metal complex displaying antibiofilm activity against *M. abscessus*. Indeed, metal complexes made of gold, silver, copper or cadmium-containing sulfonamides have recently been shown to display similar properties against a variety of NTM [46,47]. Given the relatively high concentration of zinc, magnesium, calcium and iron found in the sputum of persons with CF and non-CF bronchiectasis [48], this observation provides a basis for the development of innovative therapeutics and adjunct therapeutics directed against difficult-to-cure NTM pulmonary infections.

4. Materials and Methods

4.1. Bacterial Strains and Culture Media

Reference strains *Mabs* ATCC 19977 and *Mmas* CIP 108297 were obtained from the ATCC and CIP collections, respectively. *M. abscessus* subsp. *abscessus* and *M. abscessus* subsp. *massiliense* clinical isolates, NJH9, NJH12 and NJH18 were from persons with CF at National Jewish Health (Denver, CO, USA) [11]. *M. abscessus* subsp. *massiliense* clinical isolate 1239 was from a person with CF at the Royal Papworth Hospital, Cambridge, UK [26]. *M. abscessus* strains were grown under agitation at 37 °C in Middlebrook 7H9 medium supplemented with 10% albumin-dextrose-catalase (ADC) (BD Sciences) and 0.05% Tween 80, in SCFM [11] or on Middlebrook 7H11 agar supplemented with 10% oleic acid-albumin-dextrose-catalase (OADC) (BD Sciences). To assess the impact of zinc on growth and biofilm formation, ZnSO₄ was added at different concentrations to SCFM.

4.2. Biofilm Assay

M. abscessus submerged biofilms were formed in 96-well (polystyrene, flat bottom) poly-D-lysine-coated plates in 200 µL of SCFM and monitored by crystal violet staining as described [11].

4.3. Drug-Susceptibility Testing

The minimum inhibitory concentrations (MICs) of 2-AI-based small-molecule compounds against *Mabs* ATCC 19977 and *Mmas* CIP108297 grown planktonically were determined in SCFM in a total volume of 200 µL in 96-well microtiter plates. Cultures grown to early log phase were diluted to a final concentration of 10⁶ CFU mL⁻¹ and incubated in the presence of serial dilutions of the compounds for 5 days at 37 °C. MICs were determined as the lowest concentration of 2-AI-based compound, showing no visible growth.

4.4. Membrane Permeabilization Assay

Plasma membrane permeabilization by AB-2-29 and SDS was measured with the LIVE/DEAD BacLight kit (Thermo Fisher, Waltham, MA, USA). The fluorescence of *Mabs* ATCC 19977 bacilli, either treated with DMSO (0.2% final concentration), SDS (0.2 and 0.5%) or AB-2-29 (5 and 20 µM in 0.2% DMSO final concentration) for 1 h at 37 °C, followed by incubation with LIVE/DEAD BacLight solution for 15 min at room temperature, was

measured using an excitation wavelength of 485 nm and emission wavelengths of 535 nm (green) and 615 nm (red).

4.5. Membrane Potential and Electrochemical Proton Gradient Measurements in Intact *M. abscessus* Bacilli

The effects of AB-2-29 on the transmembrane potential ($\Delta\Psi$) and transmembrane electrochemical proton gradient (ΔpH) of intact *Mabs* ATCC 19977 cells were determined by fluorescence quenching of the membrane potential-sensitive probe 3-3' Diethyloxacarbocyanine iodide ($\text{DiOC}_2(3)$) (Thermo Fisher, Waltham, MA, USA) and the pH-sensitive probe 5-chloromethyl-fluorescein diacetate (CMFDA) (Thermo Fisher, Waltham, MA, USA), respectively, as described [49].

4.6. Assay for Succinate-Driven Proton Translocation into *M. abscessus* Inverted Membrane Vesicles (IMVs)

Succinate-driven proton translocation assays with the fluorescent substrate ACMA were conducted as previously described [49] to determine the effect of AB-2-29 on the electrochemical proton gradient of *Mabs* ATCC 19977 IMVs. IMVs (0.2 mg mL^{-1} membrane proteins) were preincubated at 37°C in 10 mM HEPES-KOH pH 7.5, 100 mM KCl, 5 mM MgCl_2 containing 20 μM ACMA, and the baseline was monitored for 10 min with a Victor X5 fluorescence spectrophotometer (PerkinElmer, Waltham, MA, USA). The reaction was then initiated by adding 5 mM succinate. Upon stabilization of the signal, control compounds (nigericin), AB-2-29 or diluent (0.2% DMSO) were added, and proton translocation was monitored fluorometrically. The excitation and emission wavelengths were 419 nm and 483 nm, respectively.

4.7. RNA Extraction, Reverse Transcription and RNAseq

Two independent cultures of DMSO (0.2%)- or AB-2-29 (20 μM)-treated *Mabs* ATCC 19977 were used for transcriptomics analyses. RNA extraction, reverse transcription reactions, RNAseq library preparation and RNAseq data analysis were conducted as described previously [11].

4.8. Atomic Absorption Spectroscopy

AB-2-29 was resuspended in DMSO at a final concentration of 10 mM, and 90 μL of sample was mixed with 200 μL HNO_3 and incubated for 1 h at 80°C and overnight at 20°C . Digestions were concluded after addition of 60 μL of 30% H_2O_2 and dilution to 2 mL with water. Samples were dried overnight at 65°C and weighed on a 5-place scale. Then, samples were dry-washed overnight at 600°C , dissolved in 3.6 N HNO_3 , diluted and analyzed using an atomic absorption spectrophotometer Model 240AA (Agilent) with reference standards for each metal. DMSO alone was included as control.

4.9. Chemical Synthesis

4-(4-propoxyphenyl)-1H-imidazol-2-amine hydrochloride (AB-2-29) was synthesized as previously reported [22].

4.10. Zinc and Iron Binding Studies

DMSO- d_6 was purchased from Sigma Aldrich. $\text{Fe(II)sulfate-heptahydrate}$ and Zn(II)Cl_2 were purchased from Acros Organics. For zinc binding studies, 4-(4-propoxyphenyl)-1H-imidazol-2-amine hydrochloride was dissolved in 500 μL of DMSO- d_6 dosed with the appropriate equivalents of anhydrous Zn(II)Cl_2 . ^1H NMR spectra were obtained on a Bruker Avance spectrometer (400 MHz) at ambient temperature. For iron binding studies, 5 μL of a 10 mM stock of 4-(4-propoxyphenyl)-1H-imidazol-2-amine hydrochloride in DMSO was pipetted into 1 mL of the appropriate aqueous solution of Fe(II)SO_4 heptahydrate. The samples were vortexed thoroughly and left at ambient temperature for 20 min. The UV spectra were obtained on a SynergyHTX (BioTek, Winooski, VT, USA) multimode plate reader using a Take3 plate and BioCell (BioTek), scanning from 200 to 800 nm.

Supplementary Materials: The following are available online at <https://www.mdpi.com/article/10.3390/ijms23062950/s1>.

Author Contributions: Conceptualization, M.J., B.R.B. and C.M.; methodology, J.M.B., W.L., M.J.Z., K.H.M., E.L., C.J.W., V.C.N.d.M., C.A. and V.J.; formal analysis, J.M.B., C.J.W., W.L., M.J.Z., M.J., B.R.B. and C.M.; investigation, J.M.B., W.L., M.J.Z., K.H.M., E.L., C.J.W., V.C.N.d.M., C.A., B.A., T.V.N. and V.J.; writing—original draft preparation, M.J.; writing—review and editing, J.M.B., C.M. and M.J.; supervision, C.M. and M.J.; project administration, M.J. and C.M.; funding acquisition, M.J., C.A. and J.M.B. All authors have read and agreed to the published version of the manuscript.

Funding: This work was supported in part by a Strategic Research Centre Award (2017-SRC 010) from the UK Cystic Fibrosis Trust (to M.J.), a Research Grant from the Cystic Fibrosis Foundation (to M.J.), the National Institute of Allergy and Infectious Diseases/National Institutes of Health grants AI147326 (to M.J.) and 1 S10 RR023735-01 (Zeiss LSM 510 Laser Scanning Microscope), and the Colorado State University Libraries Open Access Research and Scholarship Fund. J.M.B. is the recipient of a Vertex Research Innovation Award. C.A. is supported by the European Union's Horizon 2020 research and innovation program under the Marie Skłodowska-Curie grant No. 845479. The content is solely the responsibility of the authors and does not necessarily represent the official views of the sponsors.

Institutional Review Board Statement: Not applicable.

Informed Consent Statement: Not applicable.

Data Availability Statement: The sequencing data described in this publication have been submitted to the NCBI gene expression omnibus (GEO) under BioProject No. PRJNA658400.

Acknowledgments: We thank the Colorado State University Next Generation Sequencing Core facility for assistance with Illumina sequencing.

Conflicts of Interest: The authors declare no conflict of interest.

References

1. Floto, R.A.; Haworth, C.S. The growing threat of nontuberculous mycobacteria in CF. *J. Cyst. Fibros.* **2015**, *14*, 1–2. [[CrossRef](#)]
2. Martiniano, S.L.; Nick, J.A.; Daley, C.L. Nontuberculous mycobacterial infections in cystic fibrosis. *Thorac. Surg. Clin.* **2019**, *29*, 95–108. [[CrossRef](#)]
3. Park, I.K.; Olivier, K.N. Nontuberculous mycobacteria in cystic fibrosis and non-cystic fibrosis bronchiectasis. *Semin. Respir. Crit. Care Med.* **2015**, *36*, 217–224. [[CrossRef](#)]
4. Daley, C.L.; Iaccarino, J.M.; Lange, C.; Cambau, E.; Wallace, R.J.; Andrejak, C.; Böttger, E.C.; Brozek, J.; Griffith, D.E.; Guglielmetti, L.; et al. Treatment of Nontuberculous Mycobacterial Pulmonary Disease: An Official ATS/ERS/ESCMID/IDSA Clinical Practice Guideline. *Clin. Infect. Dis.* **2020**, *71*, 905–913. [[CrossRef](#)]
5. Haworth, C.S.; Banks, J.; Capstick, T.; Fisher, A.J.; Gorsuch, T.; Laurensen, I.F.; Leitch, A.; Loebinger, M.R.; Milburn, H.J.; Nightingale, M.; et al. British Thoracic Society guidelines for the management of non-tuberculous mycobacterial pulmonary disease (NTM-PD). *Thorax* **2017**, *72*, ii1–ii64. [[CrossRef](#)]
6. Egorova, A.; Jackson, M.; Gavrilyuk, V.; Makarov, V. Pipeline of anti-Mycobacterium abscessus small molecules: Repurposable drugs and promising novel chemical entities. *Med. Res. Rev.* **2021**, *41*, 2350–2387. [[CrossRef](#)]
7. Maurer, F.P.; Bruderer, V.L.; Ritter, C.; Castelberg, C.; Bloemberg, G.V.; Böttger, E.C. Lack of antimicrobial bactericidal activity in mycobacterium abscessus. *Antimicrob. Agents Chemother.* **2014**, *58*, 3828–3836. [[CrossRef](#)]
8. Wu, M.-L.; Aziz, D.B.; Dartois, V.; Dick, T. NTM drug discovery: Status, gaps and the way forward. *Drug Discov. Today* **2018**, *23*, 1502–1519. [[CrossRef](#)]
9. Brown-Elliott, B.A.; Nash, K.A.; Wallace, R.J., Jr. Antimicrobial susceptibility testing, drug resistance mechanisms, and therapy of infections with nontuberculous mycobacteria. *Clin. Microbiol. Rev.* **2012**, *25*, 545–582. [[CrossRef](#)]
10. Luthra, S.; Rominski, A.; Sander, P. The Role of Antibiotic-Target-Modifying and Antibiotic-Modifying Enzymes in Mycobacterium abscessus Drug Resistance. *Front. Microbiol.* **2018**, *9*, 2179. [[CrossRef](#)]
11. Belardinelli, J.M.; Li, W.; Avanzi, C.; Angala, S.K.; Lian, E.; Wiersma, C.J.; Palčková, Z.; Martin, K.H.; Angala, B.; de Moura, V.C.N.; et al. Unique Features of Mycobacterium abscessus Biofilms Formed in Synthetic Cystic Fibrosis Medium. *Front. Microbiol.* **2021**, *12*, 743126. [[CrossRef](#)]
12. Fennelly, K.P.; Ojano-Dirain, C.; Yang, Q.; Liu, L.; Lu, L.; Progulske-Fox, A.; Wang, G.P.; Antonelli, P.; Schultz, G. Biofilm Formation by Mycobacterium abscessus in a Lung Cavity. *Am. J. Respir. Crit. Care Med.* **2016**, *193*, 692–693. [[CrossRef](#)]
13. Høiby, N. A short history of microbial biofilms and biofilm infections. *APMIS* **2017**, *125*, 272–275. [[CrossRef](#)]
14. Qvist, T.; Eickhardt, S.; Kragh, K.N.; Andersen, C.B.; Iversen, M.; Høiby, N.; Bjarnsholt, T. Chronic pulmonary disease with Mycobacterium abscessus complex is a biofilm infection. *Eur. Respir. J.* **2015**, *46*, 1823–1826. [[CrossRef](#)]

15. Ackart, D.F.; Lindsey, E.A.; Podell, B.K.; Melander, R.J.; Basaraba, R.J.; Melander, C. Reversal of Mycobacterium tuberculosis phenotypic drug resistance by 2-aminoimidazole-based small molecules. *Pathog. Dis.* **2014**, *70*, 370–378. [[CrossRef](#)]
16. Blackledge, M.S.; Worthington, R.J.; Melander, C. Biologically inspired strategies for combating bacterial biofilms. *Curr. Opin. Pharmacol.* **2013**, *13*, 699–706. [[CrossRef](#)]
17. Brackett, S.M.; Cox, K.E.; Barlock, S.L.; Huggins, W.M.; Ackart, D.F.; Bassaraba, R.J.; Melander, R.J.; Melander, C. Meridianin D analogues possess antibiofilm activity against Mycobacterium smegmatis. *RSC Med. Chem.* **2020**, *11*, 92–97. [[CrossRef](#)]
18. Cox, K.E.; Melander, C. Anti-biofilm activity of quinazoline derivatives against Mycobacterium smegmatis. *MedChemComm* **2019**, *10*, 1177–1179. [[CrossRef](#)]
19. Jeon, A.B.; Obregón-Henao, A.; Ackart, D.F.; Podell, B.K.; Belardinelli, J.M.; Jackson, M.; Nguyen, T.V.; Blackledge, M.; Melander, R.J.; Melander, C.; et al. 2-aminoimidazoles potentiate β -lactam antimicrobial activity against Mycobacterium tuberculosis by reducing β -lactamase secretion and increasing cell envelope permeability. *PLoS ONE* **2017**, *12*, e0180925. [[CrossRef](#)]
20. Martin, S.E.; Nguyen, C.M.; Basaraba, R.J.; Melander, C. Analogue synthesis reveals decoupling of antibiofilm and beta-lactam potentiation activities of a lead 2-aminoimidazole adjuvant against Mycobacterium smegmatis. *Chem. Biol. Drug Des.* **2018**, *92*, 1403–1408. [[CrossRef](#)]
21. Melander, R.J.; Melander, C. Innovative Strategies for Combating Biofilm-Based Infections. *Adv. Exp. Med. Biol.* **2015**, *831*, 69–91. [[CrossRef](#)]
22. Nguyen, T.V.; Minrovic, B.M.; Melander, R.J.; Melander, C. Identification of Anti-Mycobacterial Biofilm Agents Based on the 2-Aminoimidazole Scaffold. *ChemMedChem* **2019**, *14*, 927–937. [[CrossRef](#)]
23. Nguyen, T.V.; Peszko, M.; Melander, R.J.; Melander, C.; Worthington, R. Using 2-aminobenzimidazole derivatives to inhibit Mycobacterium smegmatis biofilm formation. *MedChemComm* **2019**, *10*, 456–459. [[CrossRef](#)]
24. Zeiler, M.J.; Melander, R.J.; Melander, C.C. Second-Generation Meridianin Analogues Inhibit the Formation of Mycobacterium smegmatis Biofilms and Sensitize Polymyxin-Resistant Gram-Negative Bacteria to Colistin. *ChemMedChem* **2020**, *15*, 1672–1679. [[CrossRef](#)]
25. Nguyen, T.V.; Blackledge, M.S.; Lindsey, E.A.; Minrovic, B.M.; Ackart, D.F.; Jeon, A.B.; Obregón-Henao, A.; Melander, R.J.; Basaraba, R.J.; Melander, C. The Discovery of 2-Aminobenzimidazoles That Sensitize Mycobacterium smegmatis and M. tuberculosis to beta-Lactam Antibiotics in a Pattern Distinct from beta-Lactamase Inhibitors. *Angew. Chem. Int. Ed. Engl.* **2017**, *56*, 3940–3944. [[CrossRef](#)]
26. Wiersma, C.J.; Belardinelli, J.M.; Avanzi, C.; Angala, S.K.; Everall, I.; Angala, B.; Kendall, E.; De Moura, V.C.N.; Verma, D.; Benoit, J.; et al. Cell Surface Remodeling of Mycobacterium abscessus under Cystic Fibrosis Airway Growth Conditions. *ACS Infect. Dis.* **2020**, *6*, 2143–2154. [[CrossRef](#)]
27. Frei, R.; Breitbach, A.S.; Blackwell, H.E. 2-Aminobenzimidazole Derivatives Strongly Inhibit and Disperse Pseudomonas aeruginosa Biofilms. *Angew. Chem. Int. Ed.* **2012**, *51*, 5226–5229. [[CrossRef](#)]
28. Harris, T.L.; Worthington, R.J.; Hittle, L.E.; Zurawski, D.V.; Ernst, R.; Melander, C. Small Molecule Downregulation of PmrAB Reverses Lipid A Modification and Breaks Colistin Resistance. *ACS Chem. Biol.* **2014**, *9*, 122–127. [[CrossRef](#)]
29. Harris, T.L.; Worthington, R.J.; Melander, C. Potent Small-Molecule Suppression of Oxacillin Resistance in Methicillin-Resistant Staphylococcus aureus. *Angew. Chem. Int. Ed.* **2012**, *51*, 11254–11257. [[CrossRef](#)]
30. Milton, M.E.; Allen, C.L.; Feldmann, E.A.; Bobay, B.; Jung, D.K.; Stephens, M.D.; Melander, R.J.; Theisen, K.E.; Zeng, D.; Thompson, R.J.; et al. Structure of the Francisella response regulator QseB receiver domain, and characterization of QseB inhibition by antibiofilm 2-aminoimidazole-based compounds. *Mol. Microbiol.* **2017**, *106*, 223–235. [[CrossRef](#)]
31. Milton, M.E.; Minrovic, B.M.; Harris, D.L.; Kang, B.; Jung, D.; Lewis, C.P.; Thompson, R.J.; Melander, R.J.; Zeng, D.; Melander, C.; et al. Re-sensitizing Multidrug Resistant Bacteria to Antibiotics by Targeting Bacterial Response Regulators: Characterization and Comparison of Interactions between 2-Aminoimidazoles and the Response Regulators BfmR from Acinetobacter baumannii and QseB from Francisella spp. *Front. Mol. Biosci.* **2018**, *5*, 15. [[CrossRef](#)] [[PubMed](#)]
32. Thompson, R.J.; Bobay, B.G.; Stowe, S.D.; Olson, A.L.; Peng, L.; Su, Z.; Actis, L.A.; Melander, C.; Cavanagh, J. Identification of BfmR, a Response Regulator Involved in Biofilm Development, as a Target for a 2-Aminoimidazole-Based Antibiofilm Agent. *Biochemistry* **2012**, *51*, 9776–9778. [[CrossRef](#)] [[PubMed](#)]
33. Worthington, R.J.; Blackledge, M.S.; Melander, C. Small-molecule inhibition of bacterial two-component systems to combat antibiotic resistance and virulence. *Futur. Med. Chem.* **2013**, *5*, 1265–1284. [[CrossRef](#)] [[PubMed](#)]
34. Jeon, A.B.; Ackart, D.F.; Li, W.; Jackson, M.; Melander, R.J.; Melander, C.; Abramovitch, R.B.; Chicco, A.J.; Basaraba, R.J.; Obregón-Henao, A. 2-aminoimidazoles collapse mycobacterial proton motive force and block the electron transport chain. *Sci. Rep.* **2019**, *9*, 1513. [[CrossRef](#)]
35. Hurdle, J.G.; O’neill, A.J.; Chopra, I.; Lee, R.E. Targeting bacterial membrane function: An underexploited mechanism for treating persistent infections. *Nat. Rev. Microbiol.* **2011**, *9*, 62–75. [[CrossRef](#)]
36. Stowe, S.D.; Thompson, R.J.; Peng, L.; Su, Z.; Blackledge, M.S.; Draughn, G.L.; Coe, W.H.; Johannes, E.; Lapham, V.K.; MacKenzie, J.; et al. Membrane-permeabilizing activity of reverse-amide 2-aminoimidazole antibiofilm agents against Acinetobacter baumannii. *Curr. Drug Deliv.* **2015**, *12*, 223–230. [[CrossRef](#)]
37. Mikhaylina, A.; Ksibe, A.Z.; Scanlan, D.; Blindauer, C.A. Bacterial zinc uptake regulator proteins and their regulons. *Biochem. Soc. Trans.* **2018**, *46*, 983–1001. [[CrossRef](#)]

38. Goethe, E.; Laarmann, K.; Lührs, J.; Jarek, M.; Meens, J.; Lewin, A.; Goethe, R. Critical Role of Zur and SmtB in Zinc Homeostasis of *Mycobacterium smegmatis*. *mSystems* **2020**, *5*, e00880-19. [[CrossRef](#)]
39. Maciag, A.; Dainese, E.; Rodriguez, G.M.; Milano, A.; Provvedi, R.; Pasca, M.R.; Smith, I.; Palu, G.; Riccardi, G.; Manganeli, R. Global analysis of the *Mycobacterium tuberculosis* Zur (FurB) regulon. *J. Bacteriol.* **2007**, *189*, 730–740. [[CrossRef](#)]
40. Mrázek, J.; Xie, S. Pattern locator: A new tool for finding local sequence patterns in genomic DNA sequences. *Bioinformatics* **2006**, *22*, 3099–3100. [[CrossRef](#)]
41. Crooks, G.E.; Hon, G.; Chandonia, J.-M.; Brenner, S.E. WebLogo: A Sequence Logo Generator. *Genome Res.* **2004**, *14*, 1188–1190. [[CrossRef](#)] [[PubMed](#)]
42. Lindsey, E.A.; Brackett, C.M.; Mullikin, T.; Alcaraz, C.; Melander, C. The discovery of N-1 substituted 2-aminobenzimidazoles as zinc-dependent *S. aureus* biofilm inhibitors. *MedChemComm* **2012**, *3*, 1462–1465. [[CrossRef](#)] [[PubMed](#)]
43. Rogers, S.A.; Huigens, R.W., III; Melander, C. A 2-aminobenzimidazole that inhibits and disperses gram-positive biofilms through a zinc-dependent mechanism. *J. Am. Chem. Soc.* **2009**, *131*, 9868–9869. [[CrossRef](#)]
44. Mathuthu, E.; van Rensburg, A.J.; Du Plessis, D.; Mason, S. EDTA as a chelating agent in quantitative ¹H-NMR of biologically important ions. *Biochem. Cell Biol.* **2021**, *99*, 465–475. [[CrossRef](#)] [[PubMed](#)]
45. Ojha, A.; Hatfull, G.F. The role of iron in *Mycobacterium smegmatis* biofilm formation: The exochelin siderophore is essential in limiting iron conditions for biofilm formation but not for planktonic growth. *Mol. Microbiol.* **2007**, *66*, 468–483. [[CrossRef](#)] [[PubMed](#)]
46. Agertt, V.A.; Bonez, P.C.; Rossi, G.G.; Flores, V.D.C.; Siqueira, F.D.S.; Mizdal, C.R.; Marques, L.L.; De Oliveira, G.N.M.; De Campos, M.M.A. Identification of antimicrobial activity among new sulfonamide metal complexes for combating rapidly growing mycobacteria. *BioMetals* **2016**, *29*, 807–816. [[CrossRef](#)]
47. Bonez, P.C.; Agertt, V.A.; Rossi, G.G.; Siqueira, F.D.S.; Siqueira, J.D.; Marques, L.L.; de Oliveira, G.N.M.; Santos, R.C.V.; de Campos, M.M.A. Sulfonamides complexed with metals as mycobacterial biofilms inhibitors. *J. Clin. Tuberc. Other Mycobact. Dis.* **2021**, *23*, 100217. [[CrossRef](#)]
48. Smith, D.J.; Anderson, G.; Bell, S.; Reid, D. Elevated metal concentrations in the CF airway correlate with cellular injury and disease severity. *J. Cyst. Fibros.* **2014**, *13*, 289–295. [[CrossRef](#)]
49. Li, W.; Stevens, C.M.; Pandya, A.N.; Darzynkiewicz, Z.M.; Bhattarai, P.; Tong, W.; Gonzalez-Juarrero, M.; North, E.J.; Zgurskaya, H.I.; Jackson, M.C. Direct Inhibition of MmpL3 by Novel Antitubercular Compounds. *ACS Infect. Dis.* **2019**, *5*, 1001–1012. [[CrossRef](#)]